IEEE Open Journal of
Antennas and Propagation

Received 3 August 2021; revised 29 August 2021; accepted 3 September 2021. Date of publication 9 September 2021; date of current version 16 September 2021.

Digital Object Identifier 10.1109/OJAP.2021.3111434

Wideband and High Efficiency 64-Element RDRA Array for Radar Applications

FERAS ABUSHAKRA [1], ASEM AL-ZOUBI [2], ISSA AL-HMOUD [3], THISARA WALPITA [4] (Graduate Student Member, IEEE), AND NATHAN JEONG [1] (Senior Member, IEEE)

[1]Department of Electrical and Computer Engineering, University of Alabama, Tuscaloosa, AL 35487, USA
[2]Department of Telecommunications Engineering, Al-Yarmouk University, Irbid 21163, Jordan
[3]Department of Computational Data Science and Engineering, North Carolina A&T State University, Greensboro, NC 27401, USA
[4]Department of Electrical and Computer Engineering, North Carolina A&T State University, Greensboro, NC 27401, USA

CORRESPONDING AUTHOR: F. ABUSHAKRA (e-mail: fabushakra@crimson.ua.edu)

ABSTRACT This paper presents the capabilities of an 8×8 Rectangular Dielectric Resonator Antenna (RDRA) planar array with broad bandwidth and high gain. To improve shielding of a multi-stage feeding network, the proposed array is designed using a stripline feeding network with two different substrates. To enhance impedance matching while keeping a sufficient F/B ratio of 20 dB, the lower ground of the stripline has a smaller dimension than the upper ground plane. The proposed array covers the frequency band from 3.79 to 6.29 GHz with 50% fractional bandwidth. The peak realized gain ranges from 18 to 22 dBi, with 85% of radiation efficiency throughout the frequency of interest. The overall size and weight of the array is 215×215×14.5 mm^3 and 650 g, respectively. Furthermore, the radiation patterns appear as low as 15 dB of peak-to-side lobe level with 25 dB cross polarization level, which makes the proposed array suitable for UAS (Unmanned Aerial System) radar applications. The measurements and simulations agree considerably.

INDEX TERMS Dielectric resonator antennas, enhanced radiation pattern, high gain, high efficiency, planar array.

I. INTRODUCTION

MODERN radars integrated on a UAS can provide useful data in many industrial applications including soil moisture for smart agriculture, ice thickness and isotropy to investigate climate change over a long period [1], [2]. The UAS-mounted radar is capable of sensing much wider areas in a shorter time relative to a stationary radar. In addition, the radar on a UAS can grant access to extreme environments such as wildfire, flood, and earthquake. An antenna is a key component in transmitting electromagnetic signal to a target and receiving the returned signal. The challenge for a radar mounted on UAS is that the antenna should be able to support high gain, broad frequency bandwidth, light weight, realizable compact form factor, and mechanical robustness. Many types of antennas are widely used as a traditional solution to achieve these requirements, such as horn, Vivaldi and cavity-backed antennas [3]–[5]. A single horn antenna can be used to achieve high gain with wide bandwidth. However, the narrower main beam in the radiation pattern requires larger aperture area. In addition, the size and weight of the horn antenna make it difficult to mount on a UAS, especially at the lower frequency range. The phased array antennas are usually a good choice for communications and radar applications. However, their complex feeding networks limit the ability to develop a large number of elements without sacrificing the overall weight and size [6], [7]. The cavity-based antenna can be used in wide band applications, but the cavity distance will be larger at the lower frequency bands which requires more complex designing methods to miniaturize a large array [8]. Previously, a low weight array design was proposed using the magneto-electric (ME) dipole antenna that fed by a printed ridge gap waveguide through narrow slots with a narrow bandwidth of 16.5% [9]. Therefore, a trade-off is needed to have a design that can cover a wide bandwidth, high gain, compact size and narrow main beam. In an attempt to overcome aforementioned challenges, dielectric resonator antenna (DRA) is a good candidate for wideband, high gain and low weight antenna [10]–[12]. In [13], a feeding method based on the standing-wave was used to feed the RDRA array. The array gain was increased up to 15 dBi, by

exciting the TE_{115} mode instead of the dominant TE_{111}. A15-element RDRA array was fed by a dielectric image guide in [14]. The array covered the X-band with approximately 12 dBi gain. Other researchers introduced different designs for the 2D DRA array. In [15], a 4×4 planar RDRA was designed and excited through slot windows from a microstrip line feeder. The array revealed the gain from 15.2 to 18.4 dBi over 1.7 to 3 GHz, 55% bandwidth. Strip reflectors were used in the design to reduce the back lobe radiation up to 20 dB. An air gap between the array substrate and the back reflector was used to extend the bandwidth. Furthermore, a RDRA bandwidth was broadened by exciting two different modes (TE_{111} and TE_{113}) to achieve around 7 % impedance bandwidth [16].

In this paper, a wideband, low profile and high efficiency 64-element RDRA planar array with (8×8) arrangement is introduced. The proposed array shows a very good shielding for the large feeding network while keeping a 50% bandwidth with symmetric radiation patterns, stable gain value over the frequency of interest, high F/B ratio and strong mechanical structure that could be mounted on drones or airplane.

II. SINGLE-ELEMENT RDRA AND MUTUAL COUPLING

As the DRA radiates through the whole surface, it is important when designing a large array to make sure that the feeding network is totally isolated from it to prevent the higher cross polarization level. In [17], the DRA was placed on the top side of the substrate directly on the ground plane with a microstrip feeding network on the other side of the substrate. The design achieved a wide bandwidth up to 76 % for a 16-element array. However, the F/B ratio was around 10 dB. Later, the F/B ratio was improved by adding a reflector on the back side of the substrate with sufficient distance to ensure that the matching was not affected [15]. However, this approach increased the overall height of the array. Moreover, in [18], a low profile DRA was fed by slot aperture for 4 × 1 array. The feeder and substrate were isolated by a ground plane to achieve 15 dB of F/B ratio, yet with a narrow bandwidth of 17% from (4.35 to 5.37) GHz. Therefore, stripline feeder for an array could provide a good solution for reducing the interference between the radiators and the feeder as well as between the feeder and the other electronics components of the RF system. In this paper, a single element RDRA is designed using Rogers RO 3010 material with relative permittivity of 10.2 and dielectric loss tangent of 0.003. The RDRA has a square base with area of a^2 and height b with 13.6 and 11.5 mm, respectively, as shown in Fig. 1.

Two different substrates are used for the feedline. The upper substrate material is Rogers RO 4350 with relative permittivity of 3.66, dielectric loss tangent of 0.004 and thickness of 1.524 mm. The lower substrate is Rogers RT/Duroid 5880 with relative permittivity of 2.2, and 1.575 mm thickness. The connection between the feeder and the vertical strip ($W = 2.7$ mm, $L = 5.77$ mm) at the front face of the RDRA is conducted using a cylindrical probe with 0.5 mm radius. This probe passes through a circular

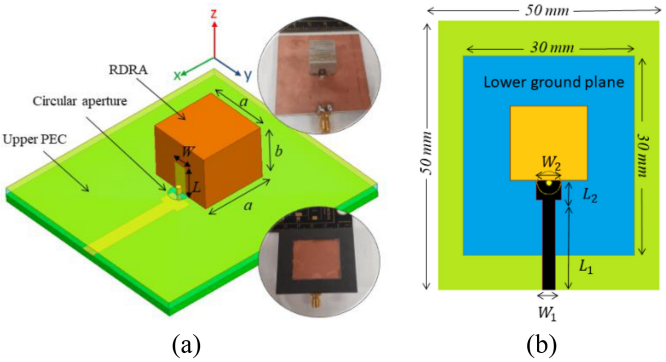

FIGURE 1. RDRA geometry. (a) 3D view with fabrication (b) top view.

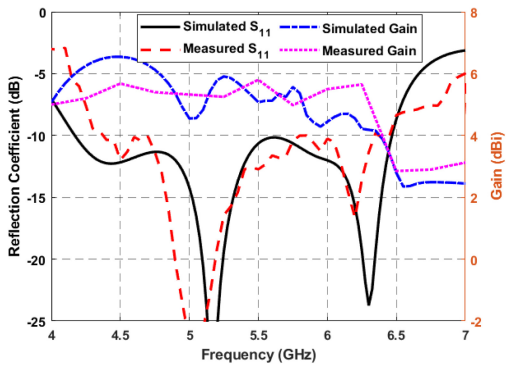

FIGURE 2. Simulated and measured reflection coefficient and gain for the single element DRA.

ground-cleared area created at the upper ground plane with 1.7 mm radius. Another ground plane with (30×30) mm^2, is assigned under the lower substrate to reduce the back-lobe radiation. The feeder's dimensions are W_1, W_2, L_1 and L_2 which correspond to 2.67, 5, 17.3 and 3.1 mm, respectively. The electromagnetic simulation is conducted with ANSYS HFSS 2020 R2 [19] to characterize the antenna performance. The results shows that the −10 dB reflection coefficient covers a frequency range from 4.21 to 6.45 GHz, while the peak realized gain is varied between 4 and 7 dBi across the operating band, as shown in Fig. 2. The measured and simulated results are in fairly good agreement.

An average radiation efficiency of 95% is achieved through the band as shown in Fig. 3. The high efficiency is one of the desired properties of the DRA which is useful to build a large array. Fig. 4 shows that the main lobe is directed along the $+z$ axis. A low cross polarization level of −20 dB and about 12 dB F/B ratio are observed at the yz-plane. The cross polarized component at the xz-plane is less than −50 dB and not shown in Fig. 4(b).

Fig. 5 shows the electric field distribution. Two resonant modes are observed across the frequency band of interest. The dominant $TE_{1\delta1}$ mode that starts from the beginning of the operating band until the second resonance at $f = 6.3$ GHz where the $TE_{2\delta1}$ starts to propagate [20].

In order to design a large array from the single RDRA design, the distance between the elements should be taken carefully into consideration. In the array radiation, the

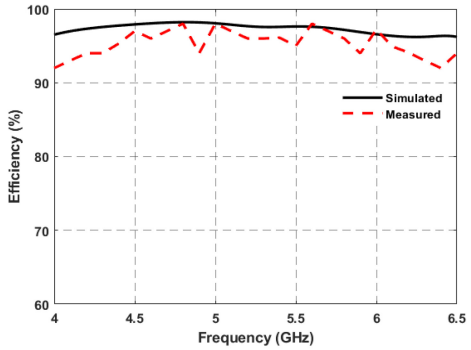

FIGURE 3. Radiation efficiency of the single-element RDRA.

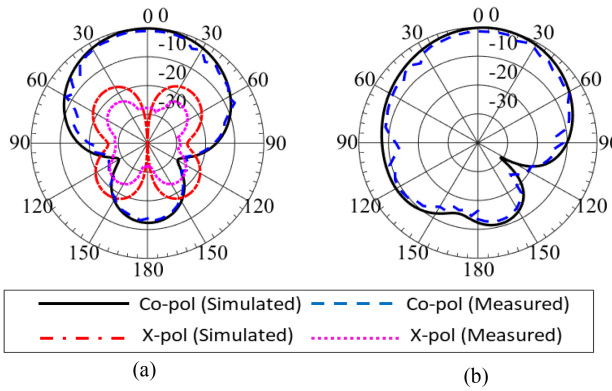

FIGURE 4. Radiation pattern of the single element RDRA at f= 4.6 GHz. (a) *yz*-plane (b) *xz*-plane.

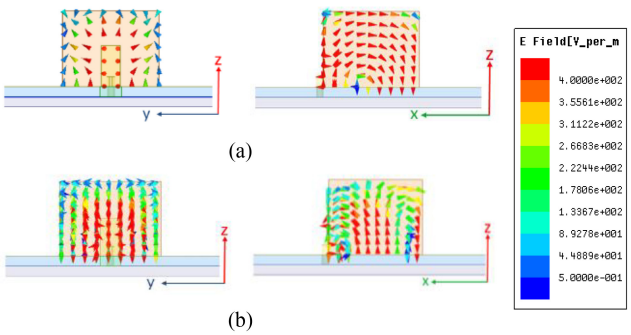

FIGURE 5. The electric field distribution in vector format (a) f = 4.6 GHz. (b) f = 6.3 GHz.

side lobes are the result of interference from nearby radiating elements. In general, to suppress the occurrence of these grating lobes, one has to make sure that the distance between the elements should be smaller than one wavelength and not less than half wavelength throughout the band. However, for wide band antennas, an appropriate element-spacing needs to be determined by placing a multiple single RDRAs excited independently alongside each other as shown in Fig. 6.

Mutual coupling is the measure of how much electromagnetic energy is coupled to each element and can be quantified with the scattering parameters, $|S_{ij}|$ where i and j are indexes of each element ($i \neq j$). After applying a parametric sweep over the distance between the elements, it is observed that

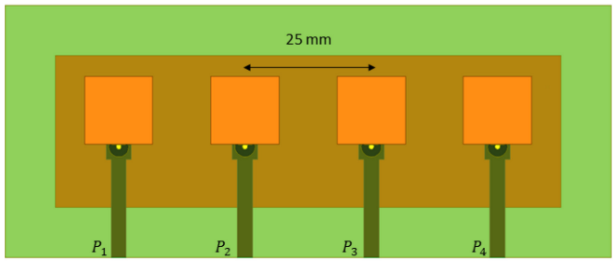

FIGURE 6. Single excitation neighbor elements RDRAs.

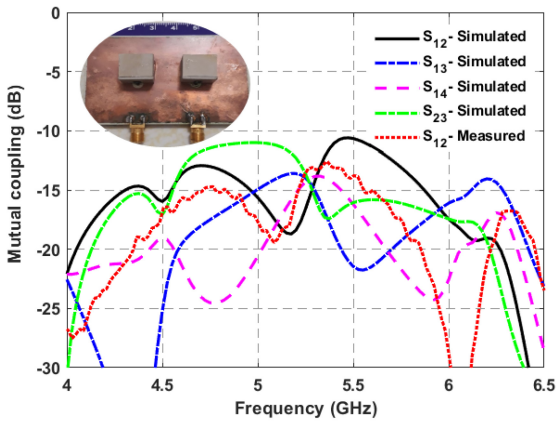

FIGURE 7. Mutual coupling between the RDRAs.

at 25 mm of the spacing, the mutual coupling between the neighboring elements through the frequency of interest is less than −13 dB except it reaches to −11 dB at f = 5.4 GHz, as shown in Fig. 7. Also, the inter-element mutual coupling represented by $|S_{23}|$ parameter shows the same level as the edge element mutual coupling, $|S_{12}|$. Thus, each DRA is spaced apart by the observed distance in both directions in the 2D array design to achieve a more symmetrical radiation pattern.

III. (8×8) PLANAR ARRAY

A cooperate stripline feeding network is designed to excite the 64-element RDRA array, as shown in Fig. 8. The multi-section power divider is shown in Fig. 8(b). The dimensions of the feeder are W_2, W_3, W_4, W_5, L_3 and L_4 which correspond to 3.2, 1.5, 1.95, 0.25, 39.3 and 8 mm, respectively. The overall size of the array substrate is 215×215 mm^2, which is considered relatively small compared to the large number of elements at this frequency range. As it could be seen, the upper ground plane has the same size of the substrate while the lower ground has a smaller size of 195×193 mm^2. The total capacitance of the stripline is a summation of the parallel-plate capacitance (C_p) and fringing capacitance (C_f) [21]. The (C_f) value will varies if the lower ground size is changed which affects the characteristic impedance. However, the (C_p) value stays the same as long as the lower ground plane covers the conductor in the middle, which is the case in this design. By reducing the ground size, the input impedance is slightly increased to match the 50 Ω port over the band.

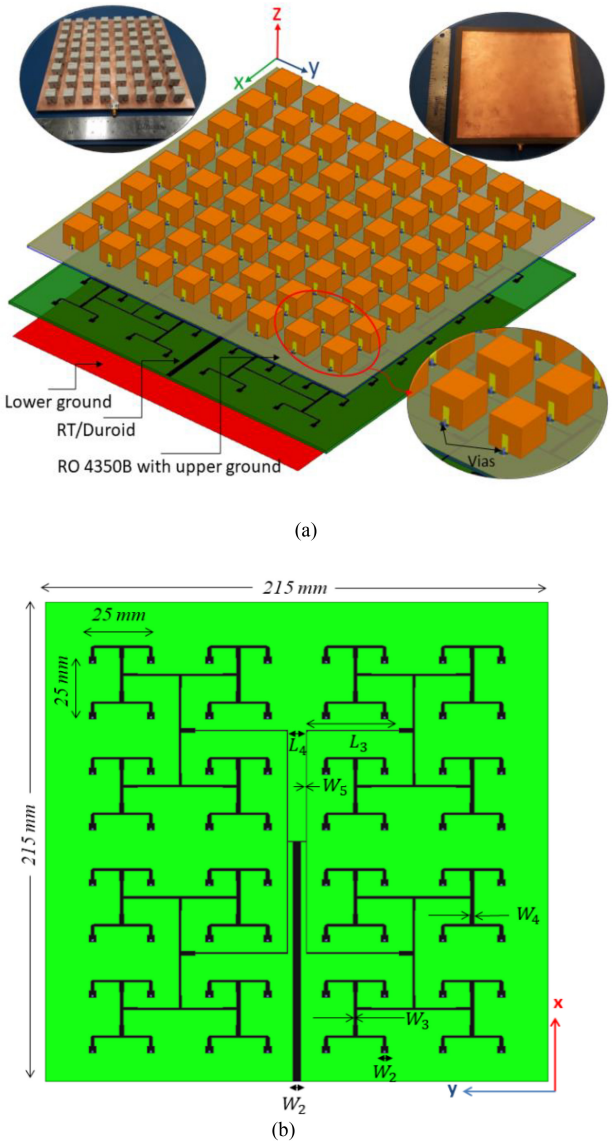

FIGURE 8. Geometry of the (8×8) planar array: (a) 3D view with the fabricated array (b) feeder.

Fig. 9 depicts the −10 dB reflection coefficient from 3.79 to 6.29 GHz, achieving 50% impedance bandwidth. The full ground plane at the bottom side of the lower substrate significantly degrades the overall matching. Also, a smaller ground plane allows the feeder radiation to adversely affect the close components of any RF system connected to the antenna, which illustrates the importance of choosing the appropriate dimensions of the ground plane to achieve the optimum bandwidth [22].

The peak realized gain varies between 18 and 22 dBi throughout the band as shown in Fig. 10(a). This gain value is considered high compared to many other large 2D arrays for radar application such as the wideband (8×8) Vivaldi array in [23], where the gain at the same frequency range of the proposed array was between (13 and 17) dBi. Some ripples in the gain value with respect to the frequency show within the operating band. However, the mean value of the

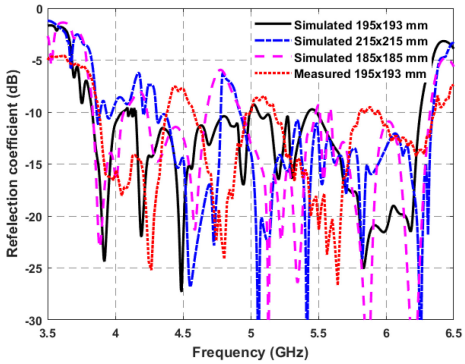

FIGURE 9. Reflection coefficient of the 8×8 proposed planar DRA array.

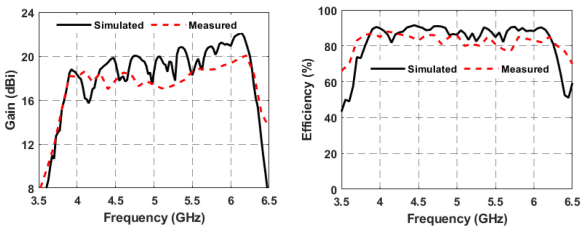

FIGURE 10. (8×8) planar array: (a) Peak realizedgain (b) Efficiency.

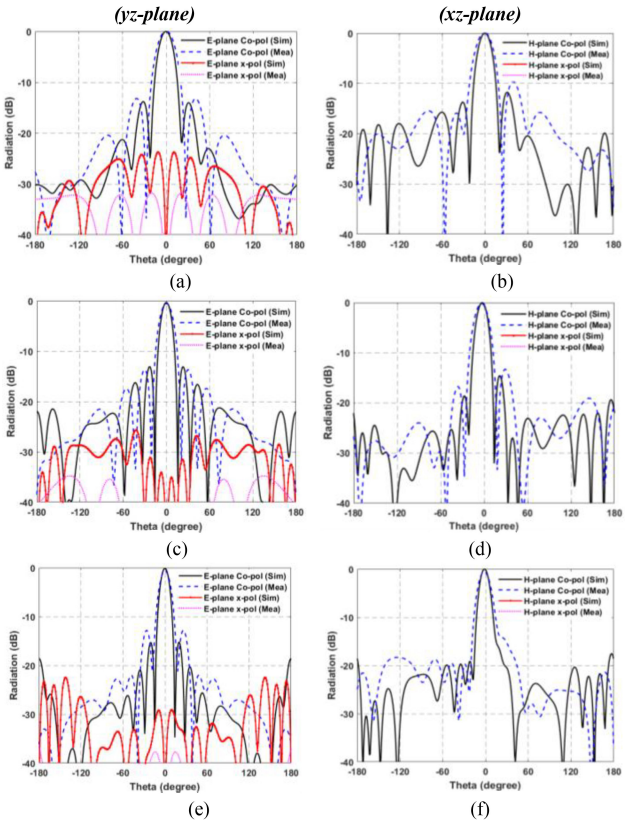

FIGURE 11. The radiation patterns for the (8×8) RDRA planar array at different frequencies: (a and b) $f = 4$ GHz, (c and d) $f = 5.1$ GHz and (e and f) $f = 6.1$ GHz.

gain is increasing from the lower to the upper frequency band, as the distance between the elements will increase with respect to the guided wavelength. The average radiation

TABLE 1. Comparison of the proposed (8×8) RDRA array with pervious designs.

Ref #	Array type/ Size (λ_o at f_L)	f (GHz)	BW (%)	Gain (dBi)	F/B (dB)
[13]	DRA (3×3) 3.3λ_o ×3.3λ_o	4.7-7.3	43.3	15	15
[15]	DRA (4×4) 1.51λ_o ×1.51λ_o	1.7-3	55.3	15.2-18.4	20
[17]	DRA (1×16) 1.3λ_o ×4.64λ_o	3.57-7.95	76	14-17	10
[18]	DRA (1×4) 0.78λ_o ×2.9λ_o	4.35-5.37	17	12	15
[This Work]	DRA (8×8) 2.7λ_o ×2.7λ_o	3.79-6.29	50	18-22	20

efficiency is 85% across the frequency of interest, as shown in Fig. 10(b). This efficiency is considered high comparing to (8×8) array [24]. Although some discrepancies between the simulated and measured results come from the tolerance in the fabrication process, the measurement and simulation are in fairly good agreement.

The radiation patterns for the 64-element array are plotted for different frequencies in Fig. 11. The results show that the cross-polarization level is less than −25 dB in the *yz*-plane and −50 dB in the *xz*- plane in the operating band. The side lobe level (SLL) is between −15 and −18 dB for both the *yz* and *xz*-plane. The HPBW varies between 13° to 18° degrees while the front to back ratio is around 20 dB through the frequency of interest. The symmetry in the radiation at the *yz*-plane is excellent but is slightly less at the *xz*-plane as the DRA has a higher electrical field intensity at the vertical strip side as illustrated in Fig. 5.

Table 1 summarizes and compares this design performance with the previous state of art. The size of the arrays is compared with respect to the free space wavelength at the lowest frequency of each design as addressed in the table. It can be seen that the array has a compact footprint compared to the other designs.

IV. CONCLUSION

A rectangular DRA planar array is demonstrated to be broadband, highly directional, efficient, and compact. A 50% of frequency bandwidth and peak realized gain of 22 dBi are achieved. The DRA feeding method and the feeder spacing between the elements are used to enhance the radiation pattern characteristics of the array. The cross polarization and side lobe level (SLL) are as low as 25 and 15 dB, respectively at the frequencies of interest. The F/B ratio of 20 dB is obtained by placing another ground plane at the bottom side of the lower substrate. The HPBW reaches to 13° at 6 GHz. The radiation patterns show a very good symmetry throughout the band. The simulated and measured results are in a good agreement.

REFERENCES

[1] R. A. Taylor *et al.*, "A prototype ultra-wideband FMCW radar for snow and soil-moisture measurements," in *Proc. IEEE Int. Geosci. Remote Sens. Symp. (IGARSS)*, Yokohama, Japan, 2019, pp. 3974–3977.

[2] N. Ghavami, I. Sotiriou, and P. Kosmas, "Limited-view prototype design for radar-based fruit imaging," in *Proc. 14th Eur. Conf. Antennas Propag. (EuCAP)*, Copenhagen, Denmarkm 2020, pp. 1–5.

[3] C. A. Balanis, *Antenna Theory Analysis and Design*. Hoboken, NJ, USA: Wiley, 2005.

[4] M. Dvorsky, H. S. Ganesh, and S. S. Prabhu, "Design and validation of an antipodal Vivaldi antenna with additional slots," *Int. J. Antennas Propag.*, vol. 2019, May 2019, Art. no. 7472186.

[5] B. S. Rao, L. Shafai, S. Sharma, V. Kane, and M. Aliamus, *Handbook of Reflector Antennas and Feed Systems Volume I: Theory and Design of Reflectors*. Boston, MA, USA: Artech House, 2013.

[6] H. J. Visser, *Array and Phased Array Antenna Basics*. Chichester, U.K.: Wiley, 2005.

[7] R. J. Mailloux, *Phased Array Antenna Handbook* (Antennas and Propagation Library), 2nd ed. Boston, MA, USA: Artech House, 2005.

[8] W. Hong, N. Behdad, and K. Sarabandi, "Size reduction of cavity-backed slot antennas," *IEEE Trans. Antennas Propag.*, vol. 54, no. 5, pp. 1461–1466, May 2006.

[9] M. S. Sorkherizi, A. Dadgarpour, and A. A. Kishk, "Planar high-efficiency antenna array using new printed ridge gap waveguide technology," *IEEE Trans. Antennas Propag.*, vol. 65, no. 7, pp. 3772–3776, Jul. 2017.

[10] D. Soren, R. Ghatak, R. K. Mishra, and D. R. Poddar, "Dielectric resonator antennas: Designs and advances," *Progr. Electromagn. Res. B*, vol. 60, pp. 195–213, Jul. 2014.

[11] S. Keyrouz and D. Caratelli, "Dielectric resonator antennas: Basic concepts, design guidelines, and recent developments at millimeter-wave frequencies," *Int. J. Antennas Propag.*, vol. 2016, Oct. 2016, Art. no. 6075680.

[12] F. Abushakra, A. Al-Zoubi, I. Uluer, and D. Hawatmeh, "Ultra-wideband E-shaped dielectric resonator antenna fed by coaxial probe and trapezoidal conductor," *Int. J. Electron. Lett.*, vol. 9, no. 2, pp. 246–255, 2021.

[13] A. A. Althuwayb *et al.*, "3-D-printed dielectric resonator antenna arrays based on standing-wave feeding approach," *IEEE Antennas Wireless Propag. Lett.*, vol. 18, pp. 2180–2183, 2019.

[14] A. S. Al-zoubi, A. A. Kishk, and A. W. Glisson, "A linear rectangular dielectric resonator antenna array fed by dielectric image guide with low cross polarization," *IEEE Trans. Antennas Propag.*, vol. 58, no. 3, pp. 697–705, Mar. 2010.

[15] M. R. Nikkhah, A. A. Kishk, and J. Rashed-Mohassel, "Wideband DRA array placed on array of slot windows," *IEEE Trans. Antenna Propag.*, vol. 63, no. 12, pp. 5382–5390, Dec. 2015.

[16] S. Chaudhuri, M. Mishra, R. S. Kshetrimayum, R. K. Sonkar, H. Chel, and V. K. Singh, "Rectangular DRA array for 24 GHz ISM-band applications," *IEEE Antennas Wireless Propag. Lett.*, vol. 19, pp. 1501–1505, 2020.

[17] F. Z. Abushakra, A. S. Al-Zoubi, and D. F. Hawatmeh, "Design and measurements of rectangular dielectric resonator antenna linear arrays," *Appl. Comput. Electromagn. Soc. J.*, vol. 33, no. 4, pp. 380–387, 2018.

[18] S. Tang, X.-Y. Wang, W.-W. Yang, and J.-X. Chen, "Wideband low-profile dielectric patch antenna and array with anisotropic property," *IEEE Trans. Antennas Propag.*, vol. 68, no. 5, pp. 4091–4096, May 2020.

[19] *HFSS: High Frequency Structure Simulator Based on the Finite Element Method, Version 19.2*, ANSYS Corp., Canonsburg, PA, USA, 2020.

[20] A. Petosa, *Dielectric Resonator Antenna Handbook*. Norwood, MA, USA: Artech House, 2007.

[21] L. Vegni, A. Toscano, and F. Bilotti, "Tapered stripline embedded in inhomogeneous media as microwave matching line," *IEEE Trans. Microw. Theory Techn.*, vol. 49, no. 5, pp. 970–978, May 2001.

[22] S. R. Best, "The significance of ground-plane size and antenna location in establishing the performance of ground-plane-dependent antennas," *IEEE Antennas Propag. Mag.*, vol. 51, no. 6, pp. 29–43, Dec. 2009.

[23] J.-B. Yan, S. Gogineni, B. Camps-Raga, and J. Brozena, "A dual-polarized 2–18-GHz Vivaldi array for airborne radar measurements of snow," *IEEE Trans. Antennas Propag.*, vol. 64, no. 2, pp. 781–785, Feb. 2016.

[24] M. A. Islam and N. C. Karmakar, "An 8×8 mm-wave LP ACMPA array for a long-range mm-Wave chipless RFID tag-sensor reader," *IEEE J. Radio Freq. Identif.*, vol. 5, no. 1, pp. 53–63, Mar. 2021.